Supporting Information

Park et al. 10.1073/pnas.1015413108

SI Materials and Methods

Mice. All procedures were approved by the Institutional Animal Care and Use Committee of Weill Cornell Medical College. Experiments were performed in C57BL/6J or *CD36*$^{0/0}$ male mice (aged 3–4 mo). For some studies, transgenic mice overexpressing the Swedish mutation of the APP Tg2576 (APP$_{Swe}$) (1) were crossed with *CD36*$^{0/0}$ mice (2). The targeted null allele is on a C57BL/6J background (N6), whereas the APP$_{Swe}$ transgene array is congenic on a 129S6 background (N18). Therefore, to minimize confounding effects attributable to background heterogeneity and genetic modifiers, experiments were performed in age-matched littermates. 129.Tg(APP$_{Swe}$)2576 mice hemizygous for the transgene array (APP$_{Swe}^{+}$/APP$_{Swe}^{-}$) were crossed with B6.129-*CD36*^{tm1Mfe} mice homozygous for the *CD36* null allele (designated $^{0/0}$) to produce *CD36*$^{0/wt}$ mice carrying the APP transgene (the transgene insertion site and *CD36* are on different chromosomes). APP$_{Swe}^{+}$ *CD36*$^{0/wt}$ F1 mice were backcrossed to *CD36*$^{0/0}$ mice to produce APP$_{Swe}^{+}$ *CD36*$^{0/0}$, APP$_{Swe}^{+}$ *CD36*$^{0/wt}$, APP$_{Swe}^{-}$ *CD36*$^{0/0}$, and APP$_{Swe}^{-}$ *CD36*$^{0/wt}$ mice. No *CD36*$^{wt/wt}$ mice were produced from this cross. To produce APP$_{Swe}^{+}$ mice and controls that are *CD36*$^{wt/wt}$ for comparison with *CD36*$^{0/0}$ and *CD36*$^{0/+}$ littermates, APP^{+} *CD36*$^{0/wt}$ and APP^{-} *CD36*$^{0/wt}$ F1 mice were intercrossed.

General Surgical Procedures. As described in detail elsewhere (3–6), mice were anesthetized with isoflurane (1–2%, vol/vol). A femoral artery was cannulated for recording of arterial pressure and collection of blood samples. In some studies, the external carotid artery ipsilateral to the cranial window was catheterized for i.c. infusion of selected agents (see below) (7). The trachea was cannulated, and mice were artificially ventilated with an O_2/N_2 mixture adjusted to provide an arterial Po_2 (Pa_{O_2}) of 120–140 mmHg (Tables S1–S4). Rectal temperature was maintained at 37 °C using a thermostatically controlled rectal probe connected to a heating pad. After surgery, isoflurane was discontinued and anesthesia was maintained with urethane (750 mg/kg, administered i.p.) and α-chloralose (50 mg/kg, administered i.p.). The level of anesthesia was monitored by testing corneal reflexes and motor responses to tail pinch.

Monitoring of CBF. The somatosensory cortex was exposed by drilling a small opening through the parietal bone (2 × 2 mm), the dura was removed, and the site was superfused with modified Ringer's solution (37 °C, pH 7.3–7.4) (3–6). CBF was continuously monitored at the site of superfusion with a laser-Doppler flow probe (Vasamedic) positioned stereotaxically near the cortical surface and connected to a computerized data acquisition system. CBF values were expressed as percent increase relative to baseline (3–6).

Detection of ROS by DHE Fluoromicrography. ROS production was measured using DHE (Molecular Probes) fluoromicrography, as previously described (5, 6, 8). DHE reacts with the ROS superoxide and is converted into ethidium and other oxidation products, which can be detected by fluorescence microscopy (5, 6, 8). DHE (2 μM) was topically superfused on the somatosensory cortex for 60 min. In some experiments, DHE superfusion was followed by cosuperfusion with Aβ (5 μM). At the end of the superfusion, the brain was removed and frozen and serial sections (thickness of 20 μm) were cut through the cortex underlying the cranial window. For analysis of DHE oxidation products, fluorescent intensities of the brain sections (15–20 sections per animal) were added, divided by the total number of pixels analyzed, and expressed as relative fluorescence units (5, 6, 8). To study ROS production in endothelial cells following i.c. infusion of $A\beta_{1–40}$, DHE was superfused cortically for 30 min, followed by a 30-min i.c. infusion of $A\beta_{1–40}$. Then, FITC-conjugated *Lycopersicon esculentum* (tomato) lectin (100 μg per 100 μL; Vector Laboratories), an endothelial marker, was infused i.c. over 5 min (9). Ten minutes later, brains were removed and frozen. Brain sections were cut and processed for DHE fluoromicrography as described above. ROS-dependent fluorescence was measured in the cells labeled with FITC–tomato lectin by confocal microscopy. For determination of ROS in endothelial cell cultures, mouse brain endothelial cells (bEND.3 cells; American Type Culture Collection) were cultured to confluence on coverslips and incubated with DHE (2 μM) for 30 min. Cells were exposed to $A\beta_{1–40}$ (300 nM; rPeptide), scrambled $A\beta_{1–40}$ (300 nM; rPeptide), $A\beta_{1–42}$ (5 μM; rPeptide), or AngII (1 μM; Sigma) for 15 min. Cultures were pretreated for 30 min with vehicle or with the ROS scavengers MnTBAP (30 μM; Calbiochem) or peg-SOD (50 U/mL; Sigma), CD36 blocking antibodies (2.5 μg/mL, Clone FA6-152; StemCell Technologies, Inc.), control IgG (2.5 μg/mL), or the NADPH oxidase peptide inhibitor gp91ds-tat (1 μM) (10). ROS-dependent fluorescence was quantified by confocal microscopy as previously described (10).

ROS and CD36 mRNA Determination in Isolated Cerebral Blood Vessels. Cerebral blood vessels were isolated from the brain surface by stripping the pia under a surgical microscope. This preparation includes large, medium, and small cerebral blood vessels. O_2^- production was assessed using L-012 (Wako Pure Chemical Industries) enhanced chemiluminescence essentially as described (11). Briefly, stripped vessels were suspended in 200 μL Krebs'/Ringer's/Hepes buffer [115 mM NaCl, 5.9 mM KCl, 2.5 mM $CaCl_2$, 1.2 mM $MgCl_2$, 1.2 mM NaH_2PO_4, 10 mM glucose, 20 mM Hepes, 25 mM $NaHCO_3$ (pH 7.35)] and transferred to a white 96-well plate. Vessels were incubated with 1 μg of antibody (FA6-152 or purified mouse IgG1 control) for 30 min, after which L-012 was added at a final concentration of 100 μM. After a 6-min equilibration period, luminescence was acquired every 2 min over 30 min in a plate luminometer (EG&G Berthold). Mean relative fluorescent light units per second was calculated over the entire observation period and subtracted from background counts obtained from wells containing L-012 but no vessels. Catalase (40U; Sigma) was added at the end of the experiment, and luminescence was acquired over a 10-min time period. Signals were reduced routinely by >80% after catalase addition. Vessels were transferred to Eppendorf tubes, collected by centrifugation, and lysed in radio-immunoprecipitation assay (RIPA) buffer. After clearance of the lysate by centrifugation, protein content was determined by DC protein assay (Bio-Rad). CD36 mRNA levels in pial vessels were determined by real-time PCR and normalized to hypoxanthine phosphoribosyltransferase mRNA (12). Relative expression levels were calculated as previously described (12).

Measurement of Plasma and Brain Aβ. Brain Aβ levels were determined using ELISA-based assays, as described previously (3–6, 13). Briefly, the left hemispheres were sonicated in 2% (wt/vol) SDS or 100 mM sodium carbonate and 50 mM NaCl (pH 6.8) with protease inhibitors and centrifuged. The supernatant contained SDS or carbonate-soluble Aβ peptides. The resulting pellets were sonicated in 70% (vol/vol) formic acid or 5 M guanidine HCl and

centrifuged as above. The formic acid extract was neutralized by a 1:20 dilution into 1 M Tris phosphate buffer (pH 8.0). $A\beta_{1-40}$ and $A\beta_{1-42}$ concentrations (pmol/g of brain tissue) were determined in supernatant (SDS-soluble) and in the formic acid extracts of the pellets (SDS-insoluble) using the BAN-50/BA-27 and BAN-50/BC005 sandwich ELISA. Alternatively, $A\beta_{1-40}$ and $A\beta_{1-42}$ concentrations were determined in supernatant (carbonate-soluble) and in the guanidine extracts of the pellet (carbonate-insoluble) using the 2G3/3D6, and 21F12/3D6 sandwich ELISA (13). For determination of plasma concentrations, plasma samples were treated with 0.5× vol/vol of 5 M guanidine HCl for 30 min at room temperature, and $A\beta_{1-40}$ concentration (pmol/mL) was determined using the 2G3/3D6 and 21F12/3D6 sandwich ELISA according to a published protocol (13).

Immunocytochemistry. Mice were deeply anesthetized with 5% isoflurane and perfused transcardially with heparinized saline, followed by 4% (wt/vol) paraformaldehyde (PFA). Brains were postfixed and sectioned with a vibratome (thickness of 40 μm). Free-floating sections were processed for double-labeling of anti-mouse CD36 IgA (1:500; BD Biosciences) with the neuronal marker MAP2 (1:500; Sigma), the endothelial cell marker CD31 (1:100; BD Biosciences), or the microglia/macrophage marker Iba1 (1 μg/mL; Wako Pure Chemical Industries). Sections were then washed and incubated with FITC-conjugated anti-mouse IgA (CD36; BD Biosciences) and cyanine dye (Cy5)-conjugated anti-rabbit IgG (MAP2 and Iba1) or anti-rat IgG (CD31) secondary antibodies (Jackson ImmunoResearch). The specificity of the labeling was established by omitting the primary antibody or by preabsorption with the antigen. The specificity for anti-mouse CD36 IgA was confirmed using control IgA and $CD36^{0/0}$ brain sections. Images were acquired using a confocal laser scanning microscope (Leica). For quantification of CD36 immunoreactivity, brain sections of Tg2576 and WT mice were processed under identical conditions and scanned at the confocal microscope using identical settings. CD36 immunoreactivity was quantified using ImageJ (National Institutes of Health). For immunocytochemistry of cerebral endothelial cell cultures, bEND.3 cells were fixed in 4% (wt/vol) PFA, washed, and processed for CD36 and CD31 or Iba1 immunocytochemistry. Confocal images were acquired as above.

Experimental Protocol for CBF Experiments. CBF recordings were started after arterial pressure and blood gases were in a steady state (Tables S1–S4). All pharmacological agents studied were dissolved in Ringer's solution, unless otherwise indicated. To study the increase in CBF produced by somatosensory activation, the whiskers were activated by side-to-side deflection for 60 s. The endothelium-dependent vasodilators ACh (10 μM; Sigma) and bradykinin (50 μM; Sigma) or the calcium ionophore A23187 (3 μM; Sigma) were topically superfused for 3–5 min, and the resulting changes in CBF were monitored. CBF responses to the smooth muscle relaxant adenosine (400 μM; Sigma) were also tested (14). Hypercapnia (P_{CO_2} to 50–60 mmHg) was induced by introducing 5% (vol/vol) CO_2 in the circuit of ventilator, and the resulting CBF increase was recorded (15). CBF responses were tested in transgene-negative mice with WT CD36 ($CD36^{wt/wt}$), Tg2576 transgenic mice with WT CD36 ($Tg2576/CD36^{wt/wt}$), Tg2576 transgenic mice lacking CD36 ($Tg2576/CD36^{0/0}$), and transgene-negative mice lacking CD36 ($CD36^{0/0}$). In some studies, after testing CBF responses with Ringer's superfusion, the superfusion solution was changed to Ringer's solution containing $A\beta_{1-40}$ (5 μM; rPeptide) or AngII (50 nM; Sigma), and responses were tested again 30–40 min later. $A\beta_{1-40}$ was freshly solubilized in DMSO to avoid subsequent peptide aggregation (15). The final concentration of DMSO (<0.2%) had no cerebrovascular effects (15). The $A\beta_{1-40}$ and AngII concentrations were selected based on previous dose–response studies (15, 16). In experiments with i.c. infusion of human $A\beta_{1-40}$, the cranial window was first superfused with Ringer's solution and CBF responses were tested. Then, vehicle or $A\beta_{1-40}$ (1 μM, 150 μL/h) was infused for 30 min and responses were tested again. The concentration of $A\beta_{1-40}$ infused was chosen to increase plasma $A\beta_{1-40}$ to a level similar to that of $Tg2576/CD36^{wt/wt}$ mice (Fig. S3*B*). In some studies, the effect of $A\beta_{1-40}$ on CBF responses was tested before and 30 min after i.c. infusion (150 μL/h) of CD36 receptor blocking antibodies (50 μg over 1.5 h, clone FA6-152; StemCell Technologies, Inc.), RAGE antibodies (50 μg over 1.5 h, polyclonal goat IgG, catalog no. AF1179; R&D Systems), or control IgG (50 μg).

Data Analysis. Data are expressed as mean ± SEM. Two-group comparisons were analyzed by the two-tailed *t* test. Multiple comparisons were evaluated by ANOVA and Tukey's test. Differences were considered statistically significant for probability values less than 0.05.

1. Hsiao K, et al. (1996) Correlative memory deficits, Abeta elevation, and amyloid plaques in transgenic mice. *Science* 274:99–102.
2. Febbraio M, et al. (1999) A null mutation in murine CD36 reveals an important role in fatty acid and lipoprotein metabolism. *J Biol Chem* 274:19055–19062.
3. Iadecola C, et al. (1999) SOD1 rescues cerebral endothelial dysfunction in mice overexpressing amyloid precursor protein. *Nat Neurosci* 2:157–161.
4. Niwa K, et al. (2000) Abeta 1-40-related reduction in functional hyperemia in mouse neocortex during somatosensory activation. *Proc Natl Acad Sci USA* 97:9735–9740.
5. Park L, et al. (2005) NADPH-oxidase-derived reactive oxygen species mediate the cerebrovascular dysfunction induced by the amyloid beta peptide. *J Neurosci* 25: 1769–1777.
6. Park L, et al. (2008) Nox2-derived radicals contribute to neurovascular and behavioral dysfunction in mice overexpressing the amyloid precursor protein. *Proc Natl Acad Sci USA* 105:1347–1352.
7. Deane R, et al. (2003) RAGE mediates amyloid-beta peptide transport across the blood-brain barrier and accumulation in brain. *Nat Med* 9:907–913.
8. Park L, et al. (2004) Exogenous NADPH increases cerebral blood flow through NADPH oxidase-dependent and -independent mechanisms. *Arterioscler Thromb Vasc Biol* 24: 1860–1865.
9. Chen Y, et al. (2004) Retroviral delivery of homeobox D3 gene induces cerebral angiogenesis in mice. *J Cereb Blood Flow Metab* 24:1280–1287.
10. Wang G, et al. (2008) Sex differences in angiotensin signaling in bulbospinal neurons in the rat rostral ventrolateral medulla. *Am J Physiol Regul Integr Comp Physiol* 295: R1149–R1157.
11. Judkins CP, et al. (2010) Direct evidence of a role for Nox2 in superoxide production, reduced nitric oxide bioavailability, and early atherosclerotic plaque formation in ApoE−/− mice. *Am J Physiol Heart Circ Physiol* 298:H24–H32.
12. Kunz A, et al. (2008) Nuclear factor-kappaB activation and postischemic inflammation are suppressed in CD36-null mice after middle cerebral artery occlusion. *J Neurosci* 28: 1649–1658.
13. Davis J, et al. (2004) Early-onset and robust cerebral microvascular accumulation of amyloid beta-protein in transgenic mice expressing low levels of a vasculotropic Dutch/Iowa mutant form of amyloid beta-protein precursor. *J Biol Chem* 279: 20296–20306.
14. Park L, Anrather J, Girouard H, Zhou P, Iadecola C (2007) Nox2-derived reactive oxygen species mediate neurovascular dysregulation in the aging mouse brain. *J Cereb Blood Flow Metab* 27:1908–1918.
15. Niwa K, Carlson GA, Iadecola C (2000) Exogenous A beta1-40 reproduces cerebrovascular alterations resulting from amyloid precursor protein overexpression in mice. *J Cereb Blood Flow Metab* 20:1659–1668.
16. Kazama K, et al. (2004) Angiotensin II impairs neurovascular coupling in neocortex through NADPH oxidase-derived radicals. *Circ Res* 95:1019–1026.

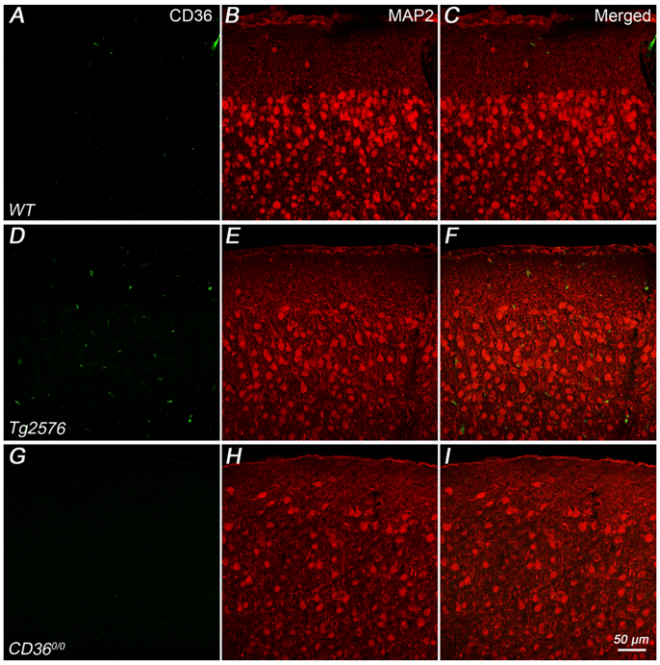

Fig. S1. CD36 immunoreactivity is not observed in neurons. CD36 immunoreactivity does not colocalize with MAP2^{+} neurons in WT mice (*A–C*) and Tg2576 transgenic mice (*D–F*). (*G–I*) CD36 immunoreactivity is not detected in CD36$^{0/0}$ mice.

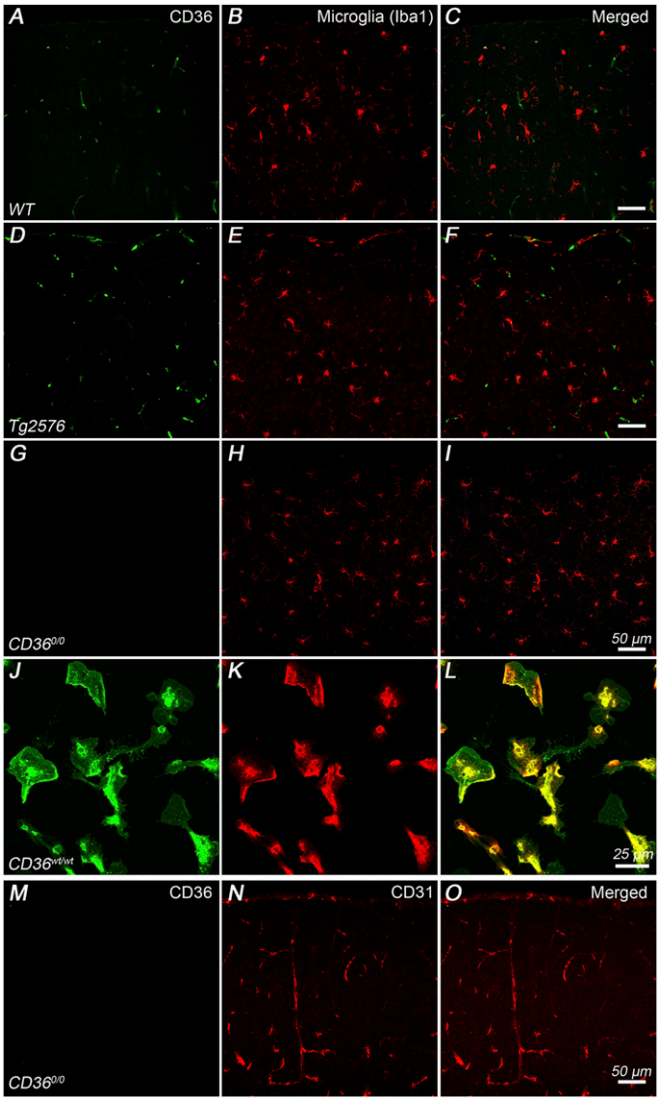

Fig. S2. CD36 immunoreactivity in microglia and endothelial cells. CD36 immunoreactivity is not detected in Iba1^{+} microglia in WT (*A*–*C*) and Tg2576 (*D*–*F*) mice. (*G*–*I*) CD36 immunoreactivity is not observed in CD36$^{0/0}$ mice. (*J*–*L*) In contrast, CD36 immunoreactivity is found in Iba^{+} microglial cultures. (*M*–*O*) CD36 immunoreactivity is not observed in CD31^{+} cells in CD36$^{0/0}$ mice.

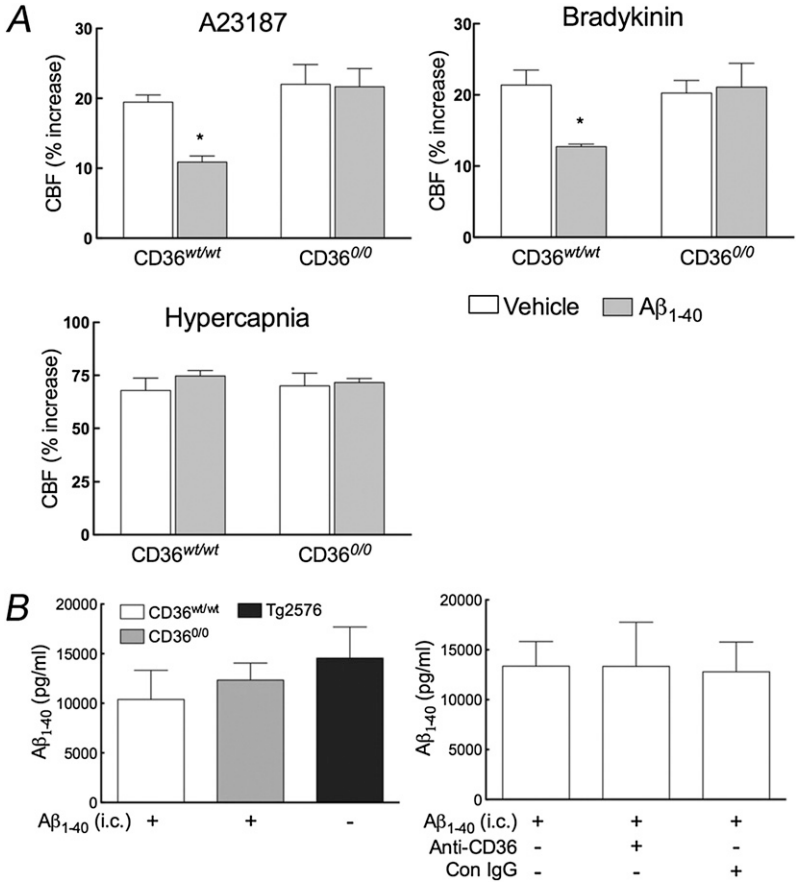

Fig. S3. (*A*) Cerebrovascular effects of $A\beta_{1-40}$ superfusion are not observed in $CD36^{0/0}$ mice. In $CD36^{wt/wt}$ mice, $A\beta_{1-40}$ (5 μM) attenuates the increase in CBF evoked by the Ca^{2+} ionophore A23187 (3 μM) and bradykinin (50 μM). These abnormalities are not observed in $CD36^{0/0}$ mice. Hypercapnia is not affected in either group. $n = 5$ per group. $^*P < 0.05$ from vehicle by ANOVA and Tukey's test. (*B*) i.c. infusion of $A\beta_{1-40}$ elevates plasma $A\beta_{1-40}$ to levels comparable to those of Tg2576. (*Left*) i.c. infusion of $A\beta_{1-40}$ (1 μM, 150 μL/h) raises plasma $A\beta_{1-40}$ in $CD36^{wt/wt}$ and $CD36^{0/0}$ to a level similar to that in Tg2576. (*Right*) Infusion of CD36 blocking antibodies (Anti-CD36) or control (Con) IgG does not influence the increase in plasma $A\beta_{1-40}$ produced by i.c. infusion of this peptide. $n = 5$ per group. $P > 0.05$ by ANOVA and Tukey's test.

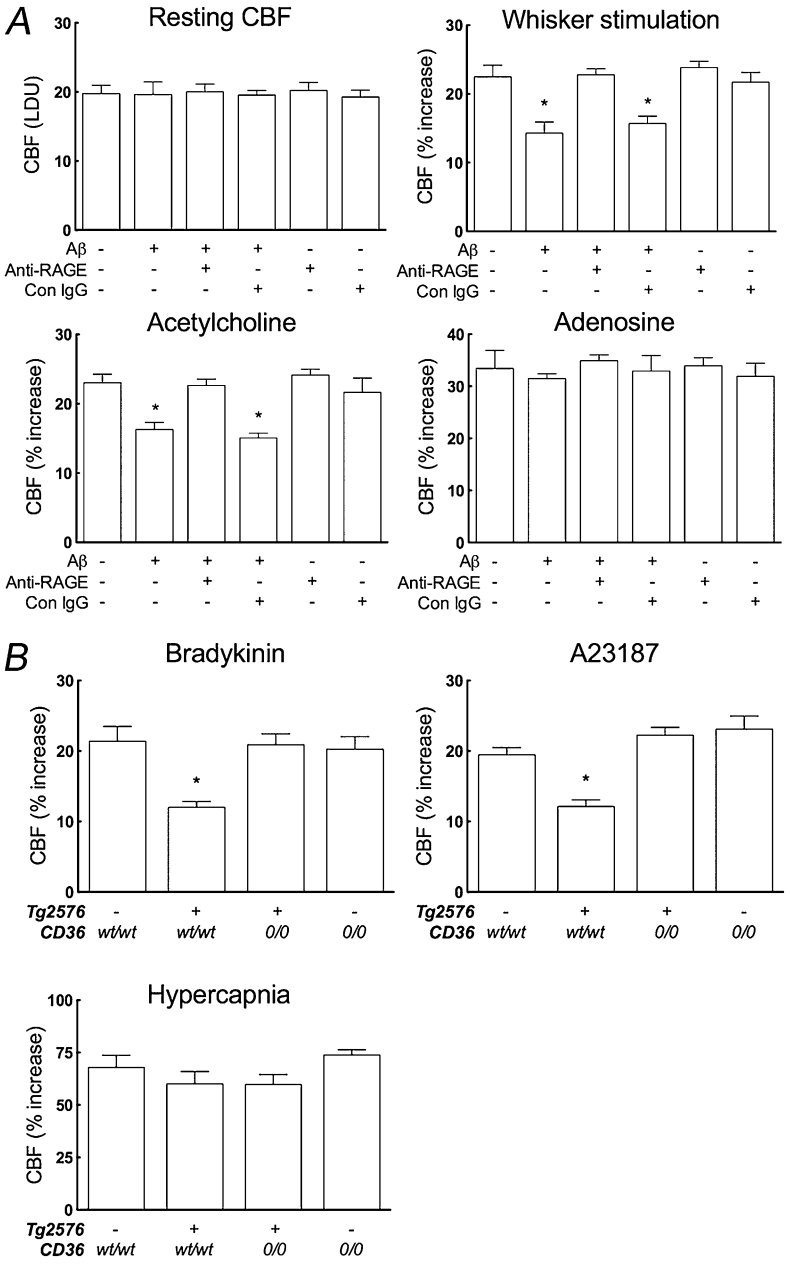

Fig. S4. (*A*) Anti-RAGE antibodies prevent cerebrovascular dysfunction induced by i.c. infusion of Aβ. Anti-RAGE antibodies were infused into the external carotid artery, and 30 min later, Aβ was added to the infusion. Anti-RAGE antibodies prevent the attenuation of the CBF response to whisker stimulation and ACh induced by i.c. infusion of Aβ. As before, Aβ does not alter the CBF response to adenosine. LDU, laser-Doppler arbitrary units. (*B*) Tg2576 mice lacking CD36 are protected from the neurovascular dysfunction. The increases in CBF evoked by bradykinin and A23187 are attenuated in Tg2576 mice expressing WT CD36. These cerebrovascular responses are not altered in Tg2576 mice lacking CD36, however. CBF responses produced by hypercapnia are not affected in any group of mice. n = 5–6 per group. *$P < 0.05$ from transgene-negative $CD36^{wt/wt}$, $Tg2576/CD36^{0/0}$, and transgene-negative $CD36^{0/0}$ by ANOVA and Tukey's test.

Table S1. Physiological variables of mice examined in Fig. 2

	Genotypes	Treatment	Stimuli	*N*	Weight, g	MAP, mmHg	P_{CO_2}, mmHg	P_{O_2}, mmHg	pH
Fig. 2	$CD36^{wt/wt}$	$A\beta_{1–40}$	Whisker, ACh, A23187	6	25.2 ± 1.8	83 ± 3	32.9 ± 0.8	131.7 ± 7.0	7.41 ± 0.01
			Bradykinin, adenosine	6		84 ± 1	31.8 ± 0.4	131.0 ± 2.0	7.40 ± 0.01
			Hypercapnia	6		84 ± 1	55.4 ± 1.3*	134.8 ± 5.0	7.23 ± 0.01*
		AngII	Whisker, ACh, adenosine	5	26.3 ± 2.2	84 ± 2	33.5 ± 2.8	135.9 ± 5.0	7.36 ± 0.02
	$CD36^{0/0}$	$A\beta_{1–40}$	Whisker, ACh, A23187	6	27.3 ± 1.5	81 ± 2	33.3 ± 1.1	130.5 ± 4.3	7.40 ± 0.01
			Bradykinin, adenosine	6		82 ± 1	31.9 ± 1.4	133.1 ± 4.1	7.38 ± 0.02
			Hypercapnia	6		82 ± 2	55.7 ± 1.6*	130.8 ± 3.8	7.23 ± 0.02*
		AngII	Whisker, ACh, adenosine	5	27.3 ± 0.8	83 ± 2	31.5 ± 1.0	132.3 ± 1.2	7.37 ± 0.01

Mean ± SEM.
*$P < 0.05$ vs. normocapnia.

Table S2. Physiological variables of mice examined in Fig. 3

	Genotypes	Treatment	Stimuli	*N*	Weight, g	MAP, mmHg	P_{CO_2}, mmHg	P_{O_2}, mmHg	pH
Fig. 3	$CD36^{wt/wt}$	Vehicle	Whisker, ACh, adenosine	5	26.1 ± 1.6	83 ± 3	33.2 ± 2.0	127.6 ± 9.1	7.36 ± 0.02
		$A\beta_{1–40}$		5		83 ± 2	30.9 ± 1.5	136.6 ± 8.1	7.38 ± 0.02
		$A\beta_{1–40}$ + anti-CD36		5		82 ± 2	30.1 ± 2.2	135.9 ± 7.5	7.36 ± 0.01
		$A\beta_{1–40}$ + control IgG		5		83 ± 2	30.6 ± 3.7	135.7 ± 4.6	7.38 ± 0.03
		Anti-CD36		5		82 ± 4	31.7 ± 2.0	132.3 ± 8.3	7.35 ± 0.02
		Control IgG		5		80 ± 4	30.5 ± 2.7	126.8 ± 8.8	7.35 ± 0.03
	$CD36^{0/0}$	$A\beta_{1–40}$		5	26.8 ± 0.6	81 ± 3	31.7 ± 1.2	128.8 ± 6.2	7.34 ± 0.01

Mean ± SEM.

Table S3. Physiological variables of mice examined in Fig. 4

	Genotypes	Stimuli	*N*	Weight, g	MAP, mmHg	P_{CO_2}, mmHg	P_{O_2}, mmHg	pH
Fig. 4	$CD36^{wt/wt}$	Whisker, ACh, A23187	6	25.7 ± 1.0	83 ± 1	33.4 ± 1.4	133.6 ± 9.8	7.40 ± 0.01
		Bradykinin, adenosine	6		84 ± 1	31.7 ± 1.3	128.4 ± 2.5	7.40 ± 0.01
		Hypercapnia	6		84 ± 3	55.9 ± 1.4*	133.7 ± 5.9	7.23 ± 0.01*
	$Tg2576/CD36^{wt/wt}$	Whisker, ACh, A23187	6	23.8 ± 0.9	81 ± 3	34.2 ± 1.8	137.9 ± 5.0	7.38 ± 0.02
		Bradykinin, adenosine	6		82 ± 1	33.8 ± 2.1	137.0 ± 5.0	7.37 ± 0.02
		Hypercapnia	6		81 ± 2	58.0 ± 2.6*	139.7 ± 3.8	7.18 ± 0.01*
	$Tg2576/CD36^{0/0}$	Whisker, ACh, A23187	6	23.3 ± 1.0	83 ± 2	32.8 ± 1.8	137.6 ± 6.7	7.38 ± 0.04
		Bradykinin, adenosine	6		83 ± 2	33.6 ± 1.5	140.2 ± 4.2	7.37 ± 0.04
		Hypercapnia	6		82 ± 2	56.2 ± 4.9*	139.4 ± 3.7	7.19 ± 0.04*
	$CD36^{0/0}$	Whisker, ACh, A23187	6	26.1 ± 0.6	82 ± 1	33.0 ± 1.7	131.0 ± 4.5	7.39 ± 0.01
		Bradykinin, adenosine	6		84 ± 1	31.9 ± 1.3	133.9 ± 4.7	7.39 ± 0.02
		Hypercapnia	6		80 ± 3	56.8 ± 3.0*	131.8 ± 4.4	7.23 ± 0.03*

Mean ± SEM.
*$P < 0.05$ vs. normocapnia.

Table S4. Physiological variables of mice examined in Fig. S4*A*

	Genotypes	Treatment	Stimuli	*N*	Weight, g	MAP, mmHg	P_{CO_2}, mmHg	P_{O_2}, mmHg	pH
Fig. S4*A*	$CD36^{wt/wt}$	$A\beta_{1–40}$, anti-RAGE	Resting, whisker, ACh, adenosine	5	27.4 ± 1.8	83 ± 4	31.1 ± 1.7	133.8 ± 7.0	7.38 ± 0.01
		$A\beta_{1–40}$ + anti-RAGE		5		84 ± 4	30.4 ± 1.6	137.0 ± 8.5	7.38 ± 0.02
		$A\beta_{1–40}$, control IgG	Resting, whisker, ACh, adenosine	5	26.6 ± 1.1	83 ± 1	32.1 ± 1.2	130.3 ± 7.4	7.38 ± 0.02
		$A\beta_{1–40}$ + control IgG		5		83 ± 2	30.2 ± 2.2	134.5 ± 6.9	7.36 ± 0.03

Mean ± SEM.